Ultrasound study of the mass decoupling of ^{4}He inert films on mesoporous silica

Junko Taniguchi,* Hideyuki Ichida, and Masaru Suzuki
Department of Engineering Science, University of Electro-Communications, Chofu, Tokyo 182-8585, Japan

(Received 12 September 2018; revised manuscript received 7 January 2019; published 29 January 2019)

We performed ultrasound measurements for ^{4}He films adsorbed on a mesoporous silica. We observed a large decrease in sound velocity with increasing temperature, accompanied by an attenuation peak. The observed dependence of the sound velocity on temperature is well explained by a thermally activated relaxation process. The magnitude of the change in sound velocity is comparable to that due to the total mass loading of ^{4}He, suggesting that the mass decoupling occurs at low temperature.

DOI: 10.1103/PhysRevB.99.024112

I. INTRODUCTION

Ultrasound (US) in MHz-order frequency is a powerful probe for studying the dislocation motion [1,2] and the vacancy diffusion [3] of solid ^{4}He. From US measurements for bulk solid ^{4}He, an anomalous nonlinear attenuation was detected, which is related to the pinning of dislocations by ^{3}He impurities [4]. For solid ^{4}He in a porous material (vycor glass), the decrease in sound velocity caused by the vacancy diffusion was reported [3]. In contrast, for ^{4}He inert film on vycor glass, the variation in sound velocity with an attenuation peak is interpreted as the interaction of ^{4}He with the two-level systems (TLS) of vycor glass [5].

On the other hand, the mass decoupling of solid films from the substrate oscillating at a MHz-order frequency has also been studied from the viewpoint of nanotribology [6]. Quartz crystal microbalance (QCM) measurements show a partial decoupling of Kr films on metal substrates [7–9].

The mass decoupling of ^{4}He inert films is an important issue [10–13]. US in MHz-order frequency enables us to measure the decoupling. This was first applied to ^{4}He inert films on hectorite [10]. It was found that mass decoupling occurs for the inert film, which disappears when the superfluid overlayer appears. Similar behavior is observed for ^{4}He films on graphite [11,12] and porous gold [13]. The relation between mass decoupling and structure change can provide us insights from a microscopic viewpoint. With this motivation, we performed ultrasound measurements for inert film ^{4}He on mesoporous silica, whose static structure is studied [14].

In the present report, first, we show the temperature dependence of sound velocity and attenuation. Next, we explain that this variation is due to mass decoupling via a thermal activation process. Finally, we discuss a possible mechanism of sticking of the film from the viewpoint of structure change in the inert film.

*tany@phys.uec.ac.jp

II. EXPERIMENTAL

A. FSM-16 sample

In the present work, we used folded sheets mesoporous materials 16 (FSM-16) [15]. It forms a nanometer-sized honeycomb structure of a straight channel without interconnection. The diameter of the channel is precisely controlled using an organic molecule as a template. Its homogeneity was confirmed by the transmission electron micrograph and the x-ray diffraction pattern [16]. The channel was 2.8 nm in diameter and 0.2–0.5 μm in length. The batch of FSM-16 used in the present work is the same as used in the previous work for superfluid [17,18] and heat capacity [19] measurements.

FSM-16 powder was formed into a pellet (ϕ6.3 mm $\times$t3 mm) by mixing with silver powder for better thermal contact, in the same manner as in the previous work [17,19]. The weight ratio of silver to FSM-16 powders was 3:1. The surface area of the pellet was determined as 39 m^2 by fitting the nitrogen vapor pressure to the BET equation. From the ^{4}He vapor pressure measurements, the areal density of the first layer completion, n_1, was determined as 9 ± 1 atoms/nm^2 [14]. The previous torsional oscillator measurements reveal that the superfluid appears above $n_C \sim 14$ atoms/nm^2, indicating that inert solid layer is formed up to n_C [17,18]. We prepared ^{4}He films of various areal densities by introducing a small dose of He gas. After an introduction, we annealed the film by raising the temperature to at most 10 K for several hours to make it uniform.

B. Ultrasound measurements

For ultrasound measurements, 10-MHz longitudinal $LiNbO_3$ transducers were bonded to both ends of the pellet. The sound velocity of the pellet (v) was measured using the pulse-echo technique with the constant phase method. The oscillating amplitude was 0.51 nm. v is described as $\sqrt{C/(\rho_{\rm sub} + \rho_{^4{\rm He}})}$, where C is the total elastic stiffness of the pellet and $\rho_{\rm sub}$ and $\rho_{^4{\rm He}}$ are the apparent densities of the substrate and ^{4}He, respectively. The numerical values in the present sample are $C = 2.47$ GPa in vacuum at the lowest

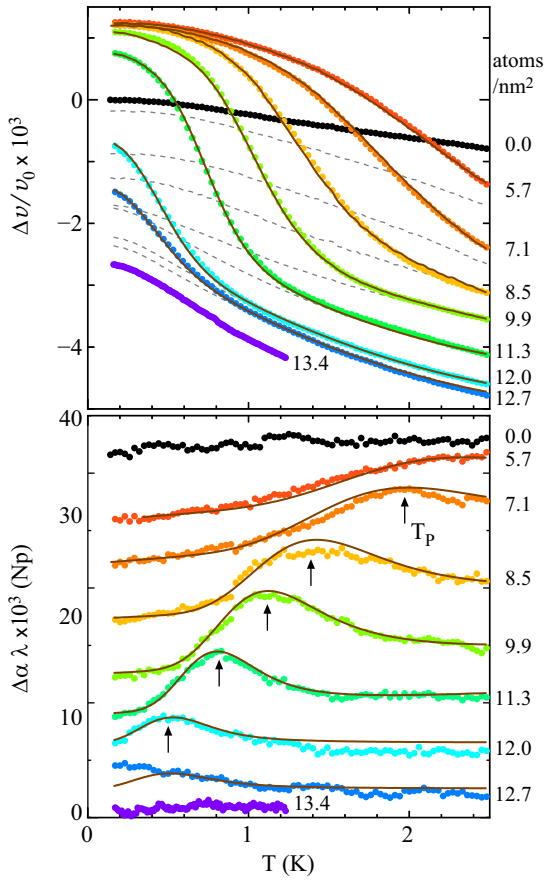

FIG. 1. Variation in the sound velocity ($\Delta v/v_0$) and attenuation ($\Delta\alpha\lambda$) as a function of temperature. For clarity, the attenuation data are shifted vertically. Figures represent the areal density in atoms/nm^2. The arrows point to T_P. The dotted curves denote estimated TLS contributions. The solid curves are fitted curves to Eqs. (3) and (4).

temperature, $\rho_{\rm sub} = 2.66 \times 10^3$ kg/m^3, and $\rho_{^4\rm He} = 28$ kg/m^3 for 10 atoms/nm^2. When C increases, the sound velocity increases. On the other hand, when the adsorbed ^{4}He moves in concert with the substrate (a sticking state), $\rho_{^4\rm He}$ increases in proportion to the amount of ^{4}He, resulting in a decrease in v. When a mass decoupling of ^{4}He from the oscillating substrate takes place, $\rho_{^4\rm He}$ decreases effectively, resulting in an increase in v from the value at the sticking state.

Figure 1 shows the sound velocity in vacuum as 0.0 atoms/nm^2. Its value at the lowest temperature, v_0 is 964 m/s, which is about half the value of other porous materials such as hectorite [20] and gelsil glass [21]. v is almost constant below about 0.4 K and then gradually decreases with increasing temperature. In glasses, the sound velocity usually increases logarithmically due to the tunneling of TLS and turns to decrease at a certain temperature due to relaxation via phonons [5,21]. The peak temperature of sound velocity ranges from ~0.1 K (hectorite) to 0.8 K (vycor glass) at around a frequency of 10 MHz, depending on material. For FSM-16, the peak temperature seems to exist at a lower temperature than the lower limit of the measurements, indicating that its crystallinity is rather high.

III. RESULTS

A. Temperature dependence

Figure 1 shows the velocity change relative to v_0 (Δv) divided by v_0, and the relative attenuation ($\Delta\alpha$) multiplied by the wavelength (λ), for various ^{4}He areal densities between 5.7 and 13.4 atoms/nm^2. At 5.7 atoms/nm^2, the sound velocity at the lowest temperature is higher than that of vacuum, implying that the adsorbed ^{4}He hardens the pellet. Hardening through the adsorption of ^{4}He was also observed for hectorite [10,22]. With increasing areal density, the value at the lowest temperature was almost constant up to 8.5 atoms/nm^2 and then turns to decrease above this areal density.

At 13.4 atoms/nm^2, where the inert solid layer is almost completed, the sound velocity shows very smooth dependence on temperature. Its slope is steeper than that of vacuum and becomes small at around the lowest temperature.

For gelsil glass, the slope of sound velocity also becomes steep as a result of the introduction of ^{4}He. This change arises from the enhancement of TLS relaxation via phonons [21]. Similarly, there is a possibility that the contribution of the relaxation is enhanced by increasing the areal density. Here we roughly estimated the contribution of the TLS in the FSM-16 to sound velocities below 12.7 atoms/nm^2 by interpolating the slope between the sound velocity in vacuum and at 13.4 atoms/nm^2. The estimated contribution is shown as dotted curves in Fig. 1 [23].

Between 5.7 and 12.7 atoms/nm^2, we observed a variation of $\Delta v/v_0$ larger than the dotted curves. At 5.7 atoms/nm^2, the sound velocity decreases rapidly with increasing temperature, with a corresponding increase in the attenuation. At 7.1 atoms/nm^2, the attenuation peak was observed at around the temperature of the steepest decrease in the sound velocity. As the areal density increases, the temperatures at which the steep decrease in the sound velocity is observed and of the attenuation peak (T_P) shift to the low temperature and disappear at 13.4 atoms/nm^2.

B. Analysis based on a thermally activated relaxation model

In this section, we show that the temperature dependence of the sound velocity and the attenuation are well explained by a model of relaxation via a thermal activation process. Generally, in the relaxation process, the sound velocity decreases steeply, accompanied by an attenuation peak, when the product of the angular frequency (ω) and the relaxation time (τ) is equal to unity. τ obeys the Arrhenius law;

$$\tau = \tau_0 \exp\left(\frac{\Delta E}{k_B T}\right). \tag{1}$$

Here ΔE is the activation energy and $1/\tau_0$ is the attempt frequency. Since the height of the observed attenuation peak is lower than that of the single relaxation, we assume that the ΔE follows the Gaussian distribution with an average activation energy, ΔE_0, and variance, σ,

$$P(\Delta E) = \frac{1}{\sqrt{2\pi\sigma^2}} \exp\left[-\frac{(\Delta E - \Delta E_0)^2}{2\sigma^2}\right]. \tag{2}$$

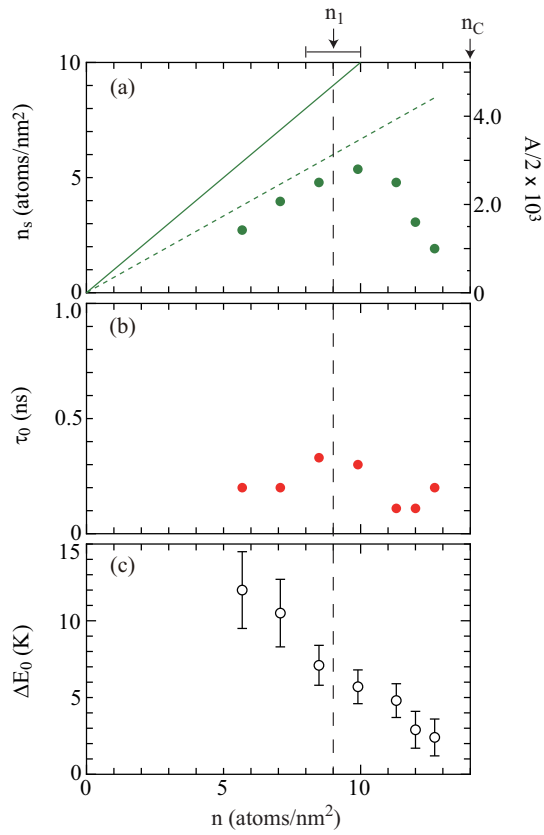

FIG. 2. Areal density dependencies of (a) n_s, (b) τ_{s0}, and (c) ΔE_0. The solid and dotted lines in (a) correspond to the total mass of the film and two-thirds of the value, respectively. The length of vertical lines in (c) corresponds to 2σ.

The variations in the sound velocity and attenuation are then described as

$$\frac{\Delta v}{v} = -\frac{A}{2}\int d(\Delta E)\frac{1}{1+\omega^2\tau^2}P(\Delta E), \tag{3}$$

$$\alpha = \pi A \int d(\Delta E)\frac{\omega\tau}{1+\omega^2\tau^2}P(\Delta E), \tag{4}$$

where $A/2$ is the amplitude of the change in $\Delta v/v$, corresponding to the difference between the solid and dotted curves at the lowest temperature in Fig. 1.

The fitted curves to the sound velocity and attenuation are shown in Fig. 1 as solid curves. As is clear from Fig. 1, the temperature dependencies are well reproduced. It should be noted that $A/2$ increases at first with increasing areal density and then turns to decrease.

The change in $\Delta v/v$ is explained as a decoupling mass. We evaluated the amount of decoupled mass (n_s) from $A/2$, using the sensitivity of the drop rate of sound velocity by ^{4}He mass loading, 5.2×10^{-4} atom^{-1} nm^2. In US measurements, almost two-thirds of the decoupled mass is detected as n_s [24]. The obtained n_s is shown as a function of areal density in Fig. 2(a). n_s increases with increasing areal density up to 10 atom/nm^2, which is just above n_1. Then it turns to decrease and approaches zero at around n_C. In the submonolayer region, n_s is close to the line corresponding to two-thirds of the total mass. This means that almost the entire film is decoupled. Similar outcomes are obtained for submonolayer ^{4}He on hectorite [10] and graphite [12].

The second fitting parameter, τ_0, is plotted against the areal density in Fig. 2(b). It ranges between 0.3 and 0.1 ns, which is several times smaller than that reported for He-hectorite [10]. The last fitting parameter, ΔE_0 is shown in Fig. 2(c). Here the magnitude of σ is presented as a length of vertical solid lines. ΔE_0 is 12 K at 5.7 atoms/nm^2 and decreases monotonously with increasing areal density to 2.4 K for 12.7 atoms/nm^2. σ also decreases correspondingly. The relaxation time τ at 1 K obtained from the fitting results decreases from 65 μs at 5.7 atoms/nm^2 to 2 ns at 12.7 atoms/nm^2. The order of τ at 12.7 atoms/nm^2 coincides with that of slip times when almost the entire ^{4}He film sticks to the oscillating substrates regardless of substrates [10,12].

From the above analysis, it is clear that a large part of the film is decoupled from the oscillating substrate at low temperature. This mass decoupling is suppressed far above T_P, due to the thermal activation process.

IV. DISCUSSION

We discuss here a possible mechanism of decoupling and sticking of the inert film. In the system of physisorbed films, the friction for the incommensurate (IC) solid configuration is generally very low, since the energy needed to move atoms is totally canceled [25]. On the other hand, the friction of fluid layer becomes larger than that of IC solid one, because of its larger deformability [7,26]. The variation from the decoupling state at low T to sticking one at high T suggests the possibility that the inert films become fluidlike at high temperatures [10].

It is of interest to examine the relation between the variation of dynamical response (from decoupling to sticking) and the static structure change suggested by the heat capacity behavior. Recent heat capacity measurements show that a Schottky-like peak appears in the ^{4}He inert film [14]. Similar heat capacity behavior was also reported for ^{4}He on vycor

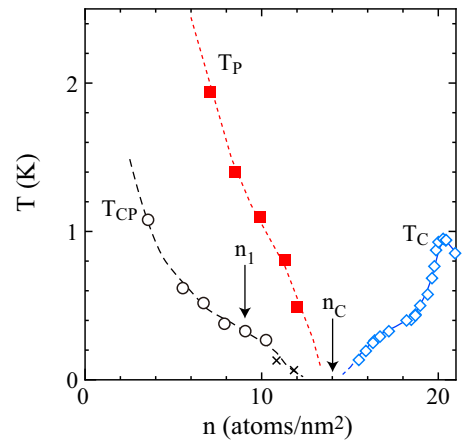

FIG. 3. Phase diagram of ^{4}He film. T_P, attenuation peak from the present work; T_{CP}, Schottky-like peak in heat capacity (○ from Ref. [14] and × from Ref. [27]); T_C, dissipation peak due to the superfluid response in the channel [18].

glass by Tait and Reppy [28]. They interpreted the peak as an excitation of atoms from a localized solid island to a delocalized two-dimensional fluid area and insisted that this fluid covers a fraction of the total surface area due to the lateral pressure generated by the corrugation of adsorption-substrate potential [29]. In the present ^{4}He-FSM system, the heat capacity behavior can be also explained in a similar way.

In Fig. 3, we plot the temperature of the Schottky-like peak, T_{CP} as a function of areal density, together with T_P and the dissipation peak temperature due to the superfluid response, T_C. Both T_P and T_{CP} decrease monotonously with increasing areal density and approache zero just below n_C, above which the superfluid overlayer appears. In addition, T_P is located at the high temperature side of T_{CP}. These indicate that the sticking of the film takes place when the fluid area is formed, which supports the possibility that the inert films become fluidlike at high temperatures. When the fluid area is locked to the substrate, the inside solid islands may be locked together to the substrate.

Next, we focus on the behavior at low temperatures where only solid exists. Below n_1, almost the entire film is decoupled, while above n_1, a part of the film sticks to the substrate even at the lowest temperature. Above n_1, a part of ^{4}He atoms are adsorbed onto the completed first layer. These atoms are expected to restrain the underlayer atoms from getting out of the minima of the potential well, resulting in a restriction of decoupling in the film.

Finally, we comment on the similarity to the mass decoupling observed in ^{4}He films on hectorite. In hectorite, the peak temperature of the attenuation is also suppressed with increasing areal density and finally disappears at the same time the superfluid appears. Furthermore, the activation energy and slip time just below n_C are in the same order. These agreements suggest that decoupling occurs in the same manner for ^{4}He film on hectorite.

V. SUMMARY

In summary, we performed ultrasound measurements for ^{4}He adsorbed on FSM-16. We observed a large variation in sound velocity accompanied by an attenuation peak. We explained that this variation is due to mass decoupling: At low temperature, the film decouples from the oscillating substrate and with increasing temperature, sticks to the oscillating substrate. In the areal density region where this behavior is observed, the fluid areas appear at high temperature. The existence of fluid areas is supposed to be relevant to sticking of the entire film.

ACKNOWLEDGMENTS

We thank S. Inagaki for the supply of FSM-16. The work was partly supported by JSPS KAKENHI Grants No. JP26400352 and No. JP18K03535.

[1] I. Iwasa, K. Araki, and H. Suzuki, J. Phys. Soc. Jpn. **46**, 1119 (1979).
[2] M. A. Paalanen, D. J. Bishop, and H. W. Dail, Phys. Rev. Lett. **46**, 664 (1981).
[3] J. R. Beamish, N. Mulders, A. Hikata, and C. Elbaum, Phys. Rev. B **44**, 9314 (1991).
[4] I. Iwasa, J. M. Goodkind, and H. Kojima, J. Phys.: Conf. Ser. **568**, 012005 (2014).
[5] N. Mulders, E. Molz, and J. R. Beamish, Phys. Rev. B **48**, 6293 (1993).
[6] J. Krim, Adv. Phys. **61**, 155 (2012).
[7] J. Krim, D. H. Solina, and R. Chiarello, Phys. Rev. Lett. **66**, 181 (1991).
[8] C. Mak and J. Krim, Phys. Rev. B **58**, 5157 (1998).
[9] L. Bruschi, A. Carlin, and G. Mistura, Phys. Rev. Lett. **88**, 046105 (2002).
[10] M. Hieda, T. Nishino, M. Suzuki, N. Wada, and K. Torii, Phys. Rev. Lett. **85**, 5142 (2000).
[11] N. Hosomi, A. Tanabe, M. Suzuki, and M. Hieda, Phys. Rev. B **75**, 064513 (2007).
[12] N. Hosomi and M. Suzuki, Phys. Rev. B **77**, 024501 (2008).
[13] J. Taniguchi, K. Wataru, K. Hasegawa, M. Hieda, and M. Suzuki, AIP Conf. Proc. **850**, 279 (2006).
[14] J. Taniguchi, K. Mikami, and M. Suzuki, arXiv:1901.06768.
[15] S. Inagaki, Y. Fukushima, and K. Kuroda, J. Chem. Soc. Chem. Commun. **22**, 680 (1993).
[16] S. Inagaki, A. Koiwai, N. Suzuki, Y. Fukushima, and K. Kuroda, Bull. Chem. Soc. Jpn. **69**, 1449 (1996).
[17] J. Taniguchi, Y. Aoki, and M. Suzuki, Phys. Rev. B **82**, 104509 (2010).
[18] K. Demura, J. Tanigcuhi, and M. Suzuki, J. Phys. Soc. Jpn. **86**, 114601 (2017).
[19] J. Taniguchi, R. Fujii, and M. Suzuki, Phys. Rev. B **84**, 134511 (2011).
[20] J. Taniguchi, H. Ichida, Y. Aoki, M. Hieda, and M. Suzuki, J. Low Temp. Phys. **148**, 791 (2007).
[21] T. Kobayashi, J. Taniguchi, A. Saito, S. Fukazawa, M. Suzki, and K. Shirahama, J. Phys. Soc. Jpn. **79**, 084601 (2010).
[22] Adsorption of ^{4}He improves the connection between FSM powders, which may cause hardening of the pellet.
[23] We estimated the value of $\Delta v/v_0$ at the lowest temperature of dotted curves in Fig. 1, from the extrapolation of its areal density dependence above 13.4 atoms/nm^2. Its ambiguity is $\sim 3 \times 10^{-4}$.
[24] When the channel axis is randomly distributed, the ratio of the surface parallel to the wave propagation to the total surface is two-thirds, which gives us the upper limit of the detectable decoupled mass.
[25] J. Frenkel and T. Kontrova, Sov. Phys. USSR **1**, 137 (1939).
[26] E. D. Smith, M. O. Robbins, and M. Cieplak, Phys. Rev. B **54**, 8252 (1996).
[27] R. Toda, M. Hieda, T. Matsushita, N. Wada, J. Taniguchi, H. Ikegami, S. Inagaki, and Y. Fukushima, Phys. Rev. Lett. **99**, 255301 (2007).
[28] R. H. Tait and J. D. Reppy, Phys. Rev. B **20**, 997 (1979).
[29] On heterogeneous substrates, it is difficult to determine whether or not the localized solid is in the IC configuration. However, the fact that almost the entire film is decoupled indicates that it is close to the IC configuration.